Momentum distributions in ^{3}He-^{4}He liquid mixtures

J. Boronat
Departament de Física i Enginyeria Nuclear, Campus Nord B4-B5, Universitat Politècnica de Catalunya, E-08034 Barcelona, Spain

A. Polls
Departament d'Estructura i Constituents de la Matèria, Universitat de Barcelona, Diagonal 647, E-08028 Barcelona, Spain

A. Fabrocini
Istituto Nazionale di Fisica Nucleare, Dipartimento di Fisica, Università di Pisa, Piazza Torricelli 2, I-56100 Pisa, Italy
(Received 28 April 1997; revised manuscript received 23 July 1997)

We present variational calculations of the one-body density matrices and momentum distributions for ^{3}He-^{4}He mixtures in the zero-temperature limit, in the framework of the correlated basis functions theory. The ground-state wave function contains two- and three-body correlations and the matrix elements are computed by (Fermi) hypernetted chain techniques. The dependence on the ^{3}He concentration (x_3) of the ^{4}He condensate fraction ($n_0^{(4)}$) and of the ^{3}He pole strength (Z_F) is studied along the $P=0$ isobar. At low ^{3}He concentrations, the computed ^{4}He condensate fraction is not significantly affected by the ^{3}He statistics. Despite the low x_3 values, Z_F is found to be quite smaller than that of the corresponding pure ^{3}He because of the strong ^{3}He-^{4}He correlations and of the overall, large total density ρ. A small increase of $n_0^{(4)}$ along x_3 is found, which is mainly due to the decrease of ρ with respect to the pure-^{4}He phase. [S0163-1829(97)03242-6]

I. INTRODUCTION

The momentum distributions (MD's) of atoms in quantum liquids is a challenging problem of fundamental interest.[1,2] They provide essential information on the correlations present in the system, which do not show up explicitly in other quantities. In the past years, accurate inelastic neutron-scattering experiments have allowed for studying several aspects of the momentum distribution in helium liquids, ^{4}He,[3,4] ^{3}He,[5] and ^{4}He-^{3}He mixtures.[6,7] However, a clean extraction of information on the helium MD's is somehow tempered by the need of a sound theoretical understanding of the final-state effects in the analysis of the dynamic structure function, even at high momentum transfers.

The theoretical methods to evaluate momentum distributions of many-body interacting, dense systems at zero temperature have also made a significant progress in recent years.[1] At present, there are results for the pure helium phases obtained within different many-body techniques, i.e., variational theory (using either integral equations[8,9] or Monte Carlo methods[10]) and almost exact stochastic methods as Green's-function Monte Carlo[11,12] (GFMC) or path-integral Monte Carlo (PIMC).[13]

The MD's of liquid ^{4}He (^{3}He) are influenced by the Bose (Fermi) statistics of the atoms. The macroscopic occupation of the zero momentum state, as given by the condensate fraction $n_0^{(4)}$, characterizes the momentum distribution of bosonic, liquid ^{4}He and it is strictly linked to its superfluid behavior. On the other hand, the discontinuity Z_F at the Fermi momentum k_F is a characteristic of the ^{3}He system when it is studied as a normal Fermi liquid.

In this paper we consider the interesting case of isotopic ^{3}He-^{4}He mixtures where, due to its fermion-boson nature, both quantities Z_F and $n_0^{(4)}$ are simultaneously present. Recent neutron-scattering experiments on helium mixtures at high momentum transfers[6,7] give additional motivation to undertake a microscopic, theoretical study of their momentum distributions and one-body density matrices. Special emphasis will be devoted to the dependence on the ^{3}He concentration x_3 of the single-particle kinetic energies of the isotopes and of Z_F and $n_0^{(4)}$.

The investigation is carried on in the framework of the variational approach. The trial wave function for the mixture contains two-body (Jastrow) and triplet correlations. This type of correlated wave function has been useful in effectively studying the pure phases.[8,9,14,15] Two of us[16] (A.P. and A.F.) derived the hypernetted and Fermi hypernetted chain (HNC/FHNC) equations for the momentum distributions of the mixtures using trial wave functions with only pair correlations. Numerical applications were carried out in the HNC/FHNC/0 approximation, i.e., neglecting the elementary diagrams. A preliminary study of the elementary diagrams for a Jastrow trial wave function was performed[17] by generalizing the scaling approximation proposed for pure phases.[8,9] Also available are variational Monte Carlo (VMC) calculations[18] with similar correlations of the analytical McMillan type. The studies of the mixture have been recently complemented with variational calculations concerning the energy and stability of the ground state,[19,20] with path-integral Monte Carlo (PIMC) analysis[21] and with microscopic correlated basis functions estimates of the inelastic neutron-scattering cross sections both at intermediate[22] and high[23] momentum transfers.

The paper is organized as follows: in Sec. II, we will present the HNC/FHNC theory to calculate $n(k)$ for mixtures described by correlated wave functions containing two- and three-body correlations. The treatment of the elementary diagrams in the so-called scaling approximation is discussed in some detail in the second part of the section. Results for

$n^{(4)}(k), n^{(3)}(k)$, and for the one-body density matrices are presented in Sec. III, together with a critical discussion of the discrepancies with the available analysis of the deep inelastic neutron-scattering measurements on mixtures, which (in contrast with our results) point to a large enhancement of the ^{4}He condensate fraction.

II. HNC/FHNC EQUATIONS FOR THE MOMENTUM DISTRIBUTION OF ^{3}He-^{4}He MIXTURES

The one-body density matrices $\rho^{(\alpha)}(\mathbf{r}_1,\mathbf{r}_1')$ ($\alpha=3,4$) for a homogeneous, isotopic mixture of N_3 ^{3}He atoms and N_4 ^{4}He atoms, described by a ground-state wave function $\Psi(1,\ldots,N_4+N_3)$ are defined as

$$\rho^{(\alpha)}(\mathbf{r}_1,\mathbf{r}_1')=\frac{N_\alpha}{\rho_\alpha}\frac{\int\Psi^*(1_\alpha,\ldots,N_4+N_3)\Psi(1_\alpha',\ldots,N_4+N_3)d\mathbf{r}_2\cdots d\mathbf{r}_{N_4+N_3}}{\int|\Psi(1,\ldots,N_4+N_3)|^2 d\mathbf{r}_1\cdots d\mathbf{r}_{N_4+N_3}}. \tag{1}$$

In homogeneous mixtures, with constant particle densities $\rho_\alpha=N_\alpha/N$, $\rho^{(\alpha)}(\mathbf{r}_1,\mathbf{r}_1')=\rho^{(\alpha)}(r)$, with $r=|\mathbf{r}_1-\mathbf{r}_1'|$. $\rho^{(\alpha)}(r)$'s satisfy the normalization conditions $\nu_\alpha\rho^{(\alpha)}(0)=1$, ν_α being the spin degeneracy ($\nu_4=1$, $\nu_3=2$). Notice that in the definition of $\rho^{(3)}(r)$ the spin variables have not been explicitly written. We will henceforth omit the subindex in the degeneracy factor and assume that it always refers to ^{3}He.

The momentum distribution of the α component, or rather the occupation probability for single-particle states with momentum $\mathbf{k}$ and given spin projection, can be obtained as the Fourier transform of the corresponding density matrix,

$$n^{(\alpha)}(k)=\delta_{\alpha4}\rho_4 n_0^{(4)}(2\pi)^3\delta(\mathbf{k})+\rho_\alpha\int d\mathbf{r}\,\exp(i\mathbf{k}\cdot\mathbf{r})[\rho^{(\alpha)}(r)-\delta_{\alpha4}n_0^{(4)}], \tag{2}$$

where $n_0^{(4)}=\rho^{(4)}(\infty)$ is the ^{4}He condensate fraction, i.e., the fraction of ^{4}He particles in the zero momentum state.

The ground state of the mixture is well described by a generalization of the correlated wave function used in the pure phases:

$$\Psi(1,\ldots,N_4+N_3)=\prod_{\alpha\leqslant\beta\leqslant\gamma=3,4}\prod_{i_\alpha\leqslant j_\beta}f^{(\alpha,\beta)}(i_\alpha,j_\beta)\times\prod_{i_\alpha\leqslant j_\beta\leqslant k_\gamma}f^{(\alpha,\beta,\gamma)}(i_\alpha,j_\beta,k_\gamma)\phi(1,\ldots,N_3). \tag{3}$$

$\phi(1,\ldots,N_3)$ is the Slater determinant of plane waves corresponding to the Fermi component of the mixture, and $f^{(\alpha,\beta)}(i_\alpha,j_\beta)$ ($f^{(\alpha,\beta,\gamma)}(i_\alpha,j_\beta,k_\gamma)$) are the two (three)-body correlation functions involving two (three) particles of types α,β (α,β,γ), respectively. Similar trial wave functions have been used in previous works to study the structure and energetic ground-state properties of ^{3}He-^{4}He mixtures.[16,19,20]

A cluster analysis of $\rho^{(\alpha)}(r)$ in powers of $\omega^{(\alpha,\beta)}\equiv f^{(\alpha,\beta)}-1$, $h^{(\alpha,\beta)}\equiv[f^{(\alpha,\beta)}]^2-1$, $\omega^{(\alpha,\beta,\gamma)}\equiv f^{(\alpha,\beta,\gamma)}-1$ and $h^{(\alpha,\beta,\gamma)}\equiv[f^{(\alpha,\beta,\gamma)}]^2-1$, as that carried out in the pure phases,[24,25] gives the following structural decomposition for $\rho^{(\alpha)}(r)$:

$$\rho^{(\alpha)}(r)=n_0^{(\alpha)}N^{(\alpha)}(r), \tag{4}$$

where massive resummations of the diagrams, as defined in Refs. 8, 9, 16, 25, may be performed in practice by using HNC/FHNC techniques.[16,20,26]

The strength factor $n_0^{(\alpha)}$ is given by

$$n_0^{(\alpha)}=\exp[2\Gamma_\omega^{(\alpha)}-\Gamma_d^{(\alpha)}] \tag{5}$$

and

$$N^\alpha(r)=\left[\delta_{\alpha4}+\delta_{\alpha3}\left(\frac{1}{\nu}l(k_Fr)-N^{(3)}_{\omega_c\omega_c}(r)-E^{(3)}_{\omega_c\omega_c}(r)\right)\right]\times\exp[N^{(\alpha)}_{\omega\omega}(r)+E^{(\alpha)}_{\omega\omega}(r)] \tag{6}$$

sums up all the irreducible diagrams with external points 1_α and $1_\alpha'$. In Eq. (6), $l(x)=3j_1(x)/x$ is the Slater function and $k_F=(6\pi^2\rho/\nu)^{1/3}$ is the ^{3}He Fermi momentum.

The functions $N_{xy}^{(\alpha)}(r)$ and $E_{xy}^{(\alpha)}(r)$ are the sums of the *nodal* and *elementary* diagrams contributions, respectively. The evaluation of the nodal functions $N_{xy}^{(\alpha)}(r)$, in the context of the HNC/FHNC approach, is discussed in Appendix A, which also contains the explicit expressions of the $\Gamma_{\omega,d}^{(\alpha)}$ factors.

The momentum distributions are computed via the density matrices by Eq. (2). We thus get

$$n^{(4)}(k)=(2\pi)^3\rho_4 n_0^{(4)}\delta(\mathbf{k})+\rho_4 n_0^{(4)}\int d\mathbf{r}\,\exp[i\mathbf{k}\cdot\mathbf{r}]\times\{\exp[N^{(4)}_{\omega\omega}(r)+E^{(4)}_{\omega\omega}(r)]-1\}, \tag{7}$$

and

$$n^{(3)}(k)=n_0^{(3)}[n_c(k)+\Theta(k_F-k)n_d(k)], \tag{8}$$

where

$$n_d(k)=1-\widetilde{X}_{cc}+2\widetilde{X}_{\omega_c c}+\frac{\widetilde{X}^2_{\omega_c c}}{1-\widetilde{X}_{cc}} \tag{9}$$

and

$$n_c(k)=-\frac{\widetilde{X}^2_{\omega_c c}}{1-\widetilde{X}_{cc}}-\rho_3\int d\mathbf{r}\,\exp[i\mathbf{k}\cdot\mathbf{r}]\{(\exp[N^{(3)}_{\omega\omega}(r)+E^{(3)}_{\omega\omega}(r)]-1)[-l(k_F r)/\nu+N^{(3)}_{\omega_c\omega_c}(r)+E^{(3)}_{\omega_c\omega_c}(r)]+E^{(3)}_{\omega_c\omega_c}(r)\}. \quad (10)$$

$X_{yc}=g_{yc}-N_{yc}+l/\nu$ for $y=\omega_c$, c and $\widetilde{X}_{xy}(k)$ stands for the Fourier transform

$$\widetilde{X}_{xy}(k)=\rho_3\int d\mathbf{r}\,e^{i\mathbf{k}\cdot\mathbf{r}}X_{xy}(r). \quad (11)$$

The strength factor $n_0^{(4)}$ is the asymptotic value of the ^{4}He one-body density matrix, $\rho^{(4)}(r\to\infty)=n_0^{(4)}$ and corresponds to the ^{4}He condensate fraction. The decomposition of $n^{(3)}(k)$ in a continuous $[n_c(k)]$ and a discontinuous $[n_d(k)]$ piece explicitly links the discontinuity of $n^{(3)}(k)$ at k_F, Z_F, to $n_d(k_F)$ by

$$Z_F=n_0^{(3)}n_d(k_F). \quad (12)$$

Scaling approximation for the elementary diagrams

The HNC/FHNC equations can be solved once a given prescription for the contributions of the elementary diagrams has been given. However, as no exact method to compute them is presently known, at least in the frame of the integral equations, one has to resort to some approximation. Among the available schemes[27–29] we have chosen the scaling approximation (SA), developed for both the energy and the one-body density matrix of pure phases,[8,9,14,15] and satisfactorily reproducing VMC calculations. Although the number of elementary diagrams in the mixture is much larger, it is straightforward to generalize the pure phases scaling approximation to our case.

The SA is based on the evaluation of the four-points elementary diagrams constructed with the combinations of the distribution functions $g^{(\alpha,\beta)}_{xy}(r)$ allowed by diagrammatic rules, and it has already been used in the calculation of the energy and of the static structure functions of the mixture.[20] The elementary diagrams are approximated by

$$E^{(\alpha,\beta)}_{dd}(r)=E(r),\quad E^{(\alpha,\beta)}_{xy}(r)=0,$$
$$\alpha,\beta\in\{3,4\},\quad xy=[de,ee,cc], \quad (13)$$

where

$$E(r)=(1+s)E^{[4]}_g(r)+E^{[4]}_t(r). \quad (14)$$

$E^{[4]}_g(r)$ and $E^{[4]}_t(r)$ are the four-point elementary diagrams without and with explicit three-body correlations into their basic structure, respectively. These diagrams are constructed by using as internal links an *averaged* dressed correlation $\hat{g}(r)-1$,

$$\hat{g}(r)=x_4^2g^{(4,4)}(r)+2x_3x_4g^{(4,3)}(r)+x_3^2g^{(3,3)}(r), \quad (15)$$

with $x_\alpha=\rho_\alpha/\rho$. The introduction of $\hat{g}(r)$ makes feasible the calculation of $E(r)$ because it reduces drastically the high number of elementary diagrams originated by all the possible bonds between ^{3}He and ^{4}He particles. Actually, for the underlying boson-boson mixture [i.e., $\Phi(1,\ldots,N_3)=1$ in Eq. (3)] and taking the same correlation functions between all types of isotopes [average correlation approximation (ACA)], $\hat{g}(r)$ provides the exact $E^{[4]}_{g,t}(r)$. This property and the small ^{3}He concentration in the physical region of interest ($x_3<0.10$) justify the use of $\hat{g}(r)$. The scaling parameter s, Eq. (14), is determined by imposing the consistency between the Pandharipande-Bethe and the Jackson-Feenberg forms of the kinetic energy for the boson-boson mixture without triplet correlations. s is calculated for each total density and it is kept fixed when x_3 changes. This assumption is plausible because, at low ^{3}He concentrations, the statistical effects in $\hat{g}(r)$ are negligible.

The additional elementary diagrams needed for the one-body density matrices are similarly evaluated:

$$E^{(\alpha,\beta)}_{\omega d}(r)=E_{\omega d}(r),\quad E^{(\alpha,\beta)}_{yz}=0\quad (yz=\omega e,\omega_c c) \quad (16)$$

with

$$E_{\omega d}(r)=(1+s_{\omega d})E^{[4]}_{\omega d,g}(r)+E^{[4]}_{\omega d,t}(r), \quad (17)$$

and

$$E^{(\alpha)}_{\omega\omega}(r)=(1+s^{(\alpha)}_{\omega\omega})E^{[4]}_{\omega\omega,g}+E^{[4]}_{\omega\omega,t}(r), \quad (18)$$

$$E^{(3)}_{\omega_c\omega_c}(r)=(1+s_{\omega_c\omega_c})E^{[4]}_{\omega_c\omega_c,g}+E^{[4]}_{\omega_c\omega_c,t}(r). \quad (19)$$

The average distribution function

$$\hat{g}_\omega(r)=x_4^2g^{(4,4)}_{\omega d}(r)+2x_3x_4[g^{(4,3)}_{\omega d}(r)+g^{(4,3)}_{\omega e}(r)]+x_3^2[g^{(3,3)}_{\omega d}(r)+g^{(3,3)}_{\omega e}(r)] \quad (20)$$

has been used to compute the above four-point elementary diagrams.

Finally, the set of single external point elementary diagrams, appearing in the strength factors $n_0^{(\alpha)}$ expressions, are approximated, as in the pure phases,[8,9] by

$$E_x=\left(1+\frac{3}{2}s_{xd}\right)E^{[4]}_{x,g}+E^{[4]}_{x,t},\quad x=\omega,d. \quad (21)$$

As far as the factors related to the momentum distributions are concerned, we have chosen $s_{\omega d}$ by imposing $T_{\rm MD}=T_{\rm JF}$, where $T_{\rm MD}$ is the total kinetic energy obtained by integrating the momentum distribution,

$$T_{\rm MD}=\frac{\hbar^2}{2m_4}\frac{x_4}{(2\pi)^3\rho_4}\int d\mathbf{k}\,k^2n^{(4)}(k)+\frac{\hbar^2}{2m_3}\frac{x_3\nu}{(2\pi)^3\rho_3}\int d\mathbf{k}\,k^2n^{(3)}(k), \quad (22)$$

and $T_{\rm JF}$ is the ground-state expectation value of the kinetic energy operator computed by the Jackson-Feenberg identity. Moreover, the fulfillment of the normalization conditions of the momentum distributions, i.e.,

$$\frac{\nu_\alpha}{(2\pi)^3\rho_\alpha}\int d\mathbf{k}\,n_\alpha(k)=1, \quad (23)$$

equivalent to $\nu_\alpha\rho^{(\alpha)}(0)=1$, requires

$$n_0^{(\alpha)} \exp[N_{\omega\omega}^{(\alpha)}(0)+E_{\omega\omega}^{(\alpha)}(0)]=1, \tag{24}$$

$$N_{\omega_c\omega_c}^{(3)}(0)+E_{\omega_c\omega_c}^{(3)}(0)=0. \tag{25}$$

These conditions are used to determine the remaining scaling parameters $(s_{\omega\omega}^{(\alpha)}, s_{\omega_c\omega_c})$.

As a matter of fact, the use for the triplet correlated wave function of the same $s_{\omega\omega}^{(\alpha)}$ and $s_{\omega_c\omega_c}$ parameters, as determined in the Jastrow case, produces significant deviations of the above normalizations from their exact values. For this reason and to ensure the correct normalizations of the density matrices, we have recalculated the scaling factors $s_{\omega d}$, $s_{\omega\omega}^{(4)}$, $s_{\omega\omega}^{(3)}$, and $s_{\omega_c\omega_c}$ when the wave function contains three-body correlations, as in Ref. 9.

III. RESULTS

In this section we report results for the momentum distributions of ^{3}He-^{4}He liquid mixtures using the Aziz potential[30] (HFDHE2) for the variational determination of the ground-state correlations. This interaction effectively describes the equation of state of the pure phases.[12,31] The interatomic potential in isotopic mixtures is the same between any pair of particles. Based on this fact, we have used the average correlation approximation (ACA). The ACA approach, which has been carefully analyzed for the impurity problem,[32] has also been used in the past to study finite concentration helium mixtures.[20,33,34] The potential is strongly repulsive at short distances, so the correlation functions are expected to show the same short-range behaviors. Small differences can arise however at intermediate and large distances, where the interaction is weaker, because of the different masses and statistics of the isotopes. Nevertheless, ACA may well serve the purpose of studying the x_3 dependence of the momentum distributions in the mixture. In fact, for Jastrow correlated wave functions we have released the ACA, allowing for different correlations in different isotopic pairs, and these extra variational degrees of freedom have not significantly changed our results.

The two-body correlation function $f(r)$ has been taken to have an analytical form, of the McMillan type at short distance and with enough flexibility to adjust to the optimal pure ^{4}He correlation behavior in the intermediate and long ranges,

$$f(r)=\exp\left(-\frac{1}{2}\left(\frac{b}{r}\right)^5\right)\left[A+B\exp\left(-\frac{(r-D)^2}{\tau r^4}\right)\right]. \tag{26}$$

The long-range, r^{-2} behavior ensures the proper linear dependence of the ^{4}He structure function at $k\to 0$.

The $f(r)$ parameters at the ^{4}He energy variational minimum, at equilibrium density $\rho_0=0.365\sigma^{-3}$ ($\sigma=2.556$ Å), are $b=1.18\sigma$, $A=0.85$, $B=1-A$, $D=3.8$ Å, and $\tau=0.043$ Å^{-2}. B and τ are related to the experimental pure ^{4}He sound velocity c and to the low-k behavior of its static structure function by

$$\frac{B}{\tau}=\frac{m_4 c}{2\pi^2\hbar\rho_0}. \tag{27}$$

The three-body correlation function $f(r_{ij},r_{ik},r_{jk})$ has the parametrized form:[8,9,14,15]

$$f(r_{ij},r_{ik},r_{jk}) =\exp\left[-\frac{1}{2}\sum_{l=0,1}\lambda_l\sum_{\text{cyc}}\xi_l(r_{ij})\xi_l(r_{ik})P_l(\hat{r}_{ij}\cdot\hat{r}_{ik})\right], \tag{28}$$

where

$$\xi_l(r)=(r-\delta_{l0}r_{tl})\exp\left[-\left(\frac{r-r_{tl}}{\omega_{tl}}\right)^2\right]. \tag{29}$$

The values of the triplet functions parameters have been taken from Ref. 14 omitting the small $l=2$ component.

The calculations presented here are performed at the experimental values of the density along the $P=0$ isobar. In this regime, the density decreases from $\rho=\rho_0$ ($x_3=0$) to $\rho=0.3582\sigma^{-3}$ at $x_3=0.066$, corresponding to the ^{3}He maximum solubility. The partial ^{3}He density increases from zero up to $\rho_3=0.0236\sigma^{-3}$ in the same x_3 range. So, we have neglected the density dependence of the variational parameters of the correlations because of the small variations both of the total and partial densities in the region of physical interest.

Before presenting the results for the helium mixtures, it is worthwhile to study the accuracy of the scaling approximation in the case of pure ^{4}He. We have considered a correlated wave function containing McMillan two-body correlations [$A=1$, $B=0$, and $b=1.20\sigma$ in Eq. (26)] and a three-body factor given by Eq. (28). At ρ_0 we obtain $n_0^{(4)}(\mathrm{JT}_1)=0.078$ and $n_0^{(4)}(\mathrm{JT}_{01})=0.081$, where the JT_1 (JT_{01}) results include triplet correlations contributions without (with) the $l=0$ component. The corresponding energies are $E/N(\mathrm{JT}_1)=-6.55$ K, and $E/N(\mathrm{JT}_{01})=-6.58$ K. A VMC study by one of the authors (J.B.), with the same trial wave functions, gives $n_0^{(4)}(\mathrm{JT}_1)(\mathrm{VMC})=0.078$, $n_0^{(4)}(\mathrm{JT}_{01})(\mathrm{VMC})=0.082$, $E/N(\mathrm{JT}_1)(\mathrm{VMC})=-6.617$ K, and $E/N(\mathrm{JT}_{01})(\mathrm{VMC})=-6.625$ K. These results have been confirmed by an independent VMC calculation of Moroni,[35] who obtained $n_0^{(4)}=0.077$ and $E/N=-6.604$ K for the (JT_1) case.

The agreement between HNC and VMC results gives confidence in the scaling approximation to the elementary diagrams as described in the previous section, prescribing a recalculation of the scaling parameters directly associated with the momentum distribution after the inclusion of the three-body correlations. Actually, if the scaling parameters in the JT cases are the ones determined at the Jastrow level (as in Refs. 8, 36), we get $n_0^{(4)}(\mathrm{JT}_1)=0.064$ with a violation of the normalization conditions of $\sim 15\%$. In addition, the $l=0$ component of the triplet correlation has been found to have a very small effect on both the energy and condensate fraction. This finding also has been confirmed by the Moroni calculations[35] and is in contrast with that of Refs. 8, 36, where the relative change in n_0 was about 25%. Due to the small effect of the $l=0$ triplet correlation, we have omitted its contribution in all the results presented for the mixture.

The use of the semioptimized two-body correlation factor of Eq. (26) and of the $l=1$ triplet correlation lowers the energy to -6.62 K and provides $n_0^{(4)}=0.082$. The Euler

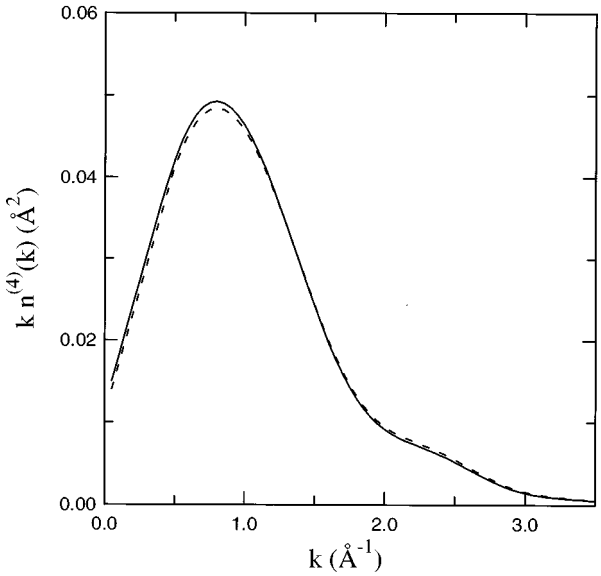

FIG. 1. Momentum distribution of the ^{4}He atoms in the mixture. The continuous line corresponds to $x_3=0.066$ ($\rho=0.3582\sigma^{-3}$) and the dashed line to pure ^{4}He at saturation density ($\rho=0.365\sigma^{-3}$). Both results are at zero pressure.

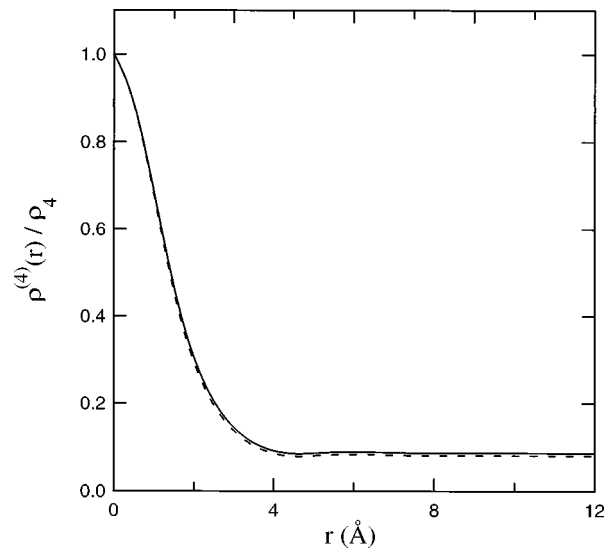

FIG. 2. One-body density matrix of the ^{4}He atoms in the mixture. The notation is the same as in Fig. 1.

Monte Carlo (EMC) result of Ref. 35, using fully optimized two- and three-body correlations in a VMC scheme, is $n_0^{(4)}(\mathrm{EMC})=0.087$. On the other hand, the DMC results of Refs. 37, 12 are $n_0^{(4)}(\mathrm{DMC})=0.072$ and $n_0^{(4)}(\mathrm{DMC})=0.084$, respectively. The difference between the two DMC results is due to the use of an extrapolated estimator which is sensitive to the overlap between the importance sampling wave function and the exact ground state. The PIMC approach of Ref. 13 provides $n_0^{(4)}(\mathrm{PIMC})=0.069$ at temperature $T=1.8$ K, with large statistical errors. As a final comment, we stress that all the above theoretical values of the ^{4}He condensate fraction are slightly lower than the latest experimental estimates of Snow *et al.*,[38] $n_0^{(4)}(\mathrm{expt})\sim 0.10$. However, as the condensate fraction, as well as the kinetic energy, is extracted by fitting the Compton scattering profile in neutron-scattering experiments at large momentum transfers, the resulting $n_0^{(4)}$ can be strongly model dependent.

We start the analysis of the mixture by studying the x_3 dependence of the ^{4}He momentum distribution. Figure 1 shows $kn^{(4)}(k)/((2\pi)^3\rho_4)$ in mixture at $x_3=0.066$ ($\rho_{\mathrm{expt}}=0.358\sigma^{-3}$) compared with that of pure ^{4}He ($\rho_4=0.365\sigma^{-3}$), both at $P=0$. The differences are small and can be explained by the slight change in density. In fact, the smaller mass of ^{3}He results in a larger zero-point motion of ^{3}He compared with ^{4}He, and therefore the total density of the mixture decreases when x_3 increases.

Figure 2 illustrates the same comparison but for the ^{4}He one-body density matrix. The asymptotic value of $\rho^{(4)}(r)$, identified with the condensate fraction, is reached at $r\sim 7$ Å. The value of $n_0^{(4)}$ in the mixture is slightly larger than in the pure phase (see also Table I) due mainly to the smaller total density of the mixture. The fermionic nature of the ^{3}He does not affect $n_0^{(4)}$. In fact, one gets the same $n_0^{(4)}$ in the boson-boson approximation, which consists of treating the ^{3}He component as a bosonic mass-3 one. Furthermore, if ACA is assumed, the boson-boson approximation yields a $n_0^{(4)}$ which is exactly the one of pure ^{4}He at the total density of the mixture.

The Fermi statistics makes the x_3 dependence of $n^{(3)}(k)$ more sizeable. The ^{3}He momentum distributions at $x_3=0.066$ and $x_3=0.020$ are compared in Fig. 3. The corresponding Fermi momenta are $k_F=0.235$ Å^{-1} and $k_F=0.347$ Å^{-1}, to be compared with $k_F=0.79$ Å^{-1} for pure ^{3}He at equilibrium density. The Fermi momentum and the discontinuity Z_F increase along x_3, whereas the depletion decreases (see Table I). This behavior is qualitatively explained by considering the change of both the total and partial ^{3}He densities.

$\rho^{(3)}(r)$ at $x_3=0.066$ is compared in Fig. 4 with the free fermionic case $[\nu\rho(r)/\rho=l(k_F r)]$ and with that of pure ^{3}He at the same ρ_3. In this density region it is necessary to reach large r values before $\rho^{(3)}(r)$ begins to oscillate around zero. Despite the small partial ^{3}He density, $\rho^{(3)}(r)$ is very different from those obtained both in the pure (short-dashed line) and the free (long-dashed line) cases. While the pure ^{3}He shows a density matrix very similar to the free case, the mixture $\rho^{(3)}(r)$ has a strong depletion due to the correlations with the ^{4}He atoms. This behavior translates into a corre-

TABLE I. ^{4}He condensate fraction, ^{3}He Z_F factor and partial kinetic energies in the mixtures as a function of the ^{3}He concentration at zero pressure. The first lines are the Jastrow values. The second lines include the effect of the triplet correlations.

x_3	$\rho(\sigma^{-3})$	n_0	Z	T_4/N_4 (K)	T_3/N_3 (K)
0.0	0.3648	0.091		15.06	19.99
		0.082		14.52	19.27
0.02	0.3629	0.092	0.093	14.92	20.04
		0.085	0.085	14.39	19.33
0.04	0.3609	0.094	0.094	14.79	19.99
		0.086	0.086	14.27	19.30
0.066	0.3582	0.096	0.096	14.61	19.88
		0.088	0.088	14.10	19.21

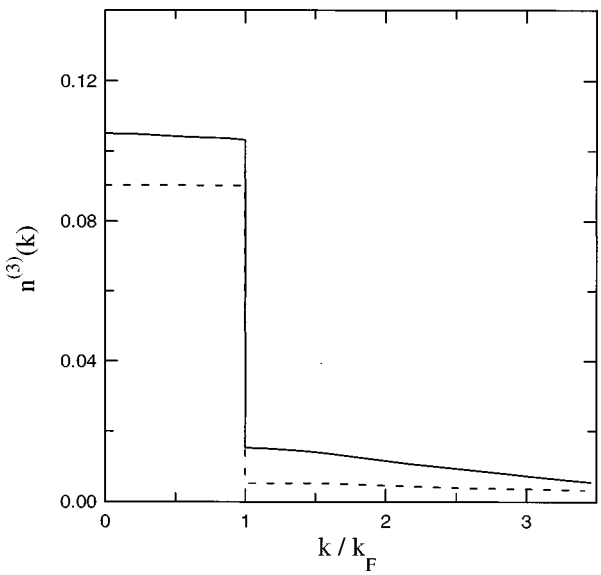

FIG. 3. ^{3}He momentum distributions in the mixture at $x_3 = 0.066$ (solid line) and $x_3 = 0.02$ (dashed line). The values of k_F are 0.347 and 0.235 Å^{-1}, respectively.

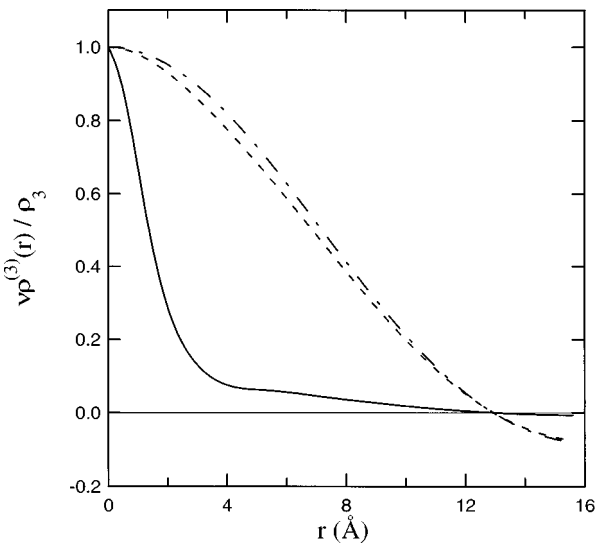

FIG. 4. One-body density matrix of the ^{3}He atoms in a $x_3 = 0.066$ mixture (solid line) compared with the free Fermi system (dash-dotted line) and pure ^{3}He (dashed line), both at the same partial density ρ_3.

spondingly large depletion of $n^{(3)}(k)$ at the origin, $n^{(3)}(k=0,\ x_3=0.066)=0.1$, while for pure ^{3}He at the same partial density as in the mixture $n^{(3)}(k=0)=0.9$. Notice that in pure ^{3}He at its equilibrium density $n(k=0)=0.5$.[9] The three density matrices have the nodes approximately at the same points, the location of the zeros being governed by the zeros of $l(k_F r)$. In fact, by taking the lowest-order term of the expansion of $\rho^{(3)}(r)$ in powers of the statistical correlation $l(k_F r)$, as done in the Wu-Feenberg expansion for the distribution function, one obtains

$$\rho^{(3)}_{\mathrm{WF}}(r)=\rho^{(3)}_B(r)\,\frac{l(k_F r)}{\nu}, \tag{30}$$

where $\rho^{(3)}_B(r)$ is the ^{3}He density matrix in the underlying boson-boson mixture. Due to the small values of x_3 in the mixture, $\rho^{(3)}_{\mathrm{WF}}(r)$ is almost indistinguishable from the exact $\rho^{(3)}(r)$.

Equation (30) explicitly decouples the statistical and dynamical correlations contributions to $\rho^{(3)}(r)$ and has also recently proved to describe quite accurately even the pure ^{3}He density matrix.[37] In this approximation, $n^{(3)}(k)$ is given by

$$n^{(3)}_{\mathrm{WF}}(k)=\frac{1}{(2\pi)^3\rho_3}\int_0^{k_F} d^3k'\,n^{(3)}_B(|\mathbf{k}-\mathbf{k}'|). \tag{31}$$

Therefore, the discontinuity Z_F coincides with the value of the condensate fraction associated with $n^{(3)}_B(k)$. The kinetic energy associated with $n^{(3)}_{\mathrm{WF}}(k)$ can be expressed as

$$\frac{T_3}{N_3}=\frac{3\hbar^2k_F^2}{10m_3}+\frac{T_{B3}}{N_3}, \tag{32}$$

where T_{B3}/N_3 is the kinetic energy associated with $n^{(3)}_B(k)$. In the ACA, the density matrices of the two components of the underlying boson-boson mixture are the same and are equal to the density matrix of pure ^{4}He considered at the total density of the mixture. As a consequence, the corresponding condensate fractions are also equal and in this model Z_F and $n^{(4)}_0$ coincide.

More detailed information on the x_3 dependence of the condensate fraction, the discontinuity of $n^{(3)}(k)$ at the Fermi surface and the kinetic energies of the two components is shown in Table I, the explicit values of $n^{(\alpha)}(k)$ being reported in Appendix B. $T_3(x_3=0)$ is the kinetic energy of one ^{3}He impurity in ^{4}He. Recent DMC (Ref. 39) and PIMC (Ref. 21) calculations predict a smaller $T_3(x_3=0)$ value of about 17.5 K. The effect of the three-body correlations is similar to that in the ^{4}He pure phase, i.e., they slightly decrease the condensate fraction and simultaneously decrease by about half a Kelvin the total kinetic energy. The condensate fraction $n^{(4)}_0$ shows a small increment with x_3. As we have mentioned before, this is mainly a consequence of the fact that the total density of the mixture slightly decreases when x_3 increases. The effect of the Fermi statistics on $n^{(4)}_0$ is almost negligible, the results of $n^{(4)}_0$ in the boson-boson approximation being equal to the ones reported in Table I.

$n^{(4)}_0$ is shown in Fig. 5 as a function of the pressure, P, for pure ^{4}He (diamonds) and for a $x_3=0.066$ mixture (circles). The condensate fraction, in both cases, decreases with pressure as a consequence of the corresponding increase of density. The density of pure ^{4}He is larger than the one of the mixture at the same pressure and therefore the condensate fraction in the mixture is larger than in ^{4}He. However, as P increases, the differences between the densities become smaller and the condensate fractions of both systems get closer.

The low values of Z_F imply a large value of the energy-dependent effective mass at the Fermi surface,

$$M_E=1-\frac{\partial}{\partial E}\,\Re\Sigma(p,E)|_{E=e_F,p=p_F}=Z_F^{-1}, \tag{33}$$

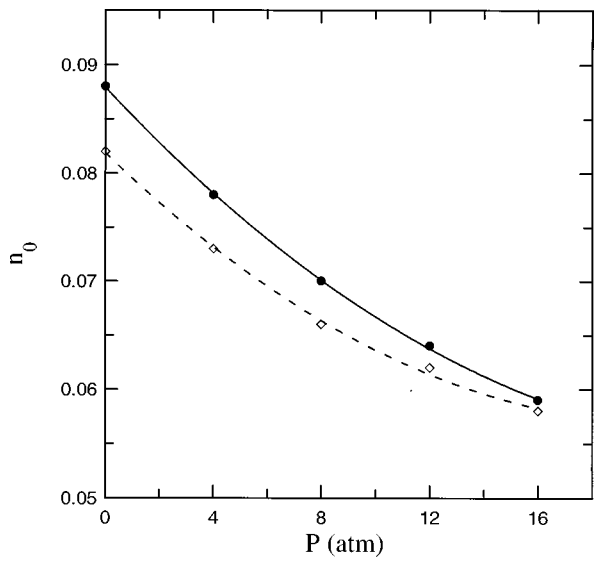

FIG. 5. Condensate fraction as a function of pressure. The diamonds and circles correspond to pure ^{4}He and to a $x_3=0.066$ mixture, respectively. The lines are guides to the eye.

where $\Sigma(p,E)$ is the self-energy of the ^{3}He atoms in the mixture. At $x_3=0.04$, $M_E=12m_3$, which is around three times larger than for pure ^{3}He at the saturation density, for which $Z_F=0.275$ and consequently $M_E=3.6m_3$.[9,37] This large value of the energy-dependent effective mass can be attributed to the correlations with the ^{4}He atoms, and implies a small value of the k-dependent effective mass in order to reproduce the total effective mass that, at those small concentrations, can be taken $m_3^*/m_3=2.3$,[40,41] i.e., the value in the impurity case.

Figure 6 shows $n^{(4)}(k)/\rho_4$ and $\nu n^{(3)}/\rho_3$ for a 6% mixture (solid and long-dashed lines, respectively) together with $n^{(4)}(k)/\rho_4$ for pure ^{4}He at the equilibrium density (short-dashed). The three momentum distributions are very close above k_F, as the large-k behavior is essentially dominated

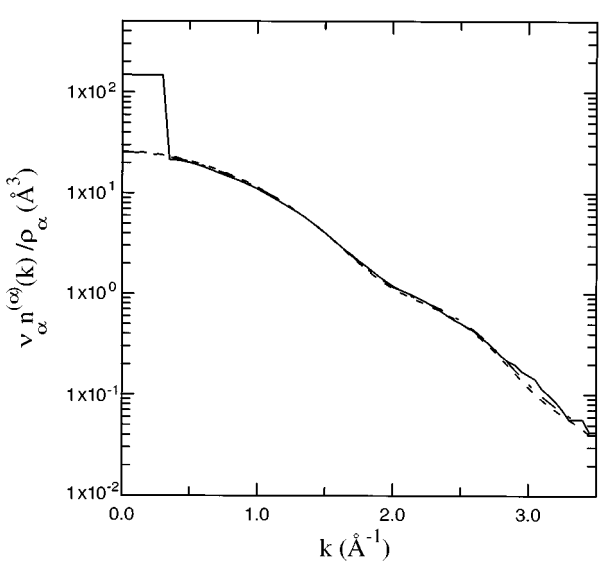

FIG. 6. Momentum distributions per particle of pure ^{4}He at equilibrium density (short-dashed), and of ^{4}He (long-dashed) and ^{3}He (solid) of a $x_3=0.066$ mixture.

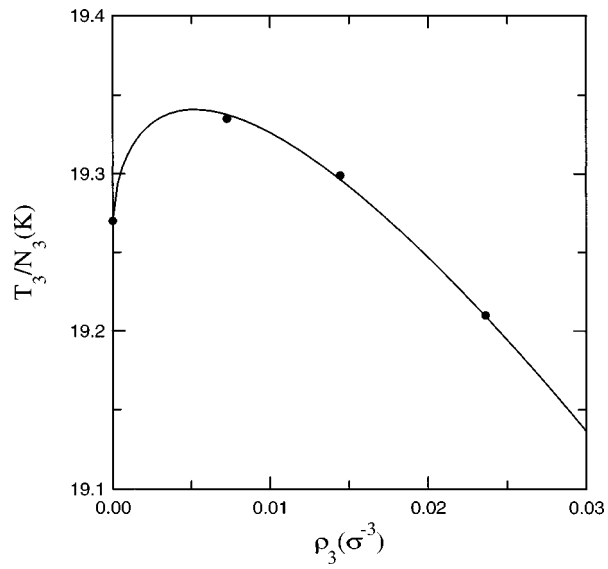

FIG. 7. ^{3}He kinetic energy as a function of ρ_3 at $P=0$. The solid line is the fit provided by Eq. (35).

by the short-range dynamical correlations. As in the pure phases, the tails of the momentum distributions ($k>3.5$ Å^{-1}) are taken to have an exponential behavior

$$n(k>3.5)=n(k=3.5)\exp(\alpha(k-3.5)), \tag{34}$$

the value of α being obtained by fitting a straight line to the $\ln n(k)$ in the range $3.0\leqslant k\leqslant 3.5$. Their contribution at $x=6.6\%$ to the total kinetic energy is $\sim 8\%$. On the other hand, the kinetic energy of the free Fermi sea (that would give an upper-bound to the contribution to T_3/N_3 below k_F) is 0.58 K. That means that more than 97% of the ^{3}He kinetic energy comes from momenta above k_F, clearly showing the importance of the correlations between ^{3}He and ^{4}He atoms.

It is also of interest to consider the dependence of T_3/N_3 on the concentration. Figure 7 gives T_3/N_3 in function of the ^{3}He partial density in the mixture along the $P=0$ isobar. Obviously, the kinetic energy ends up with the kinetic energy of pure ^{3}He (~ 12 K) which corresponds to a density value that lies out of the plot. Therefore the kinetic energy of the ^{3}He should be in average a decreasing function of the concentration except for the behavior at the origin where the term associated with the free Fermi kinetic energy dominates the overall decreasing behavior driven by the decrease of the total density. Actually, the kinetic energy in the interval considered here is well parametrized as the sum of the free-Fermi-gas energy plus a linear term describing the decrease of the kinetic energy with the density

$$\frac{T_3}{N_3}=\frac{T_3}{N_3}(\rho_3=0)-A\rho_3+\frac{3}{10}\frac{\hbar^2}{m_3}\left(\frac{6\pi^2}{\nu}\right)^{2/3}\rho_3^{2/3}. \tag{35}$$

The numerical value of the parameter A may be estimated by calculating the x_3 dependence of the kinetic energy in the underlying boson-boson mixture and it results to be $A=27.2$ Kσ^3.

IV. DISCUSSION AND CONCLUSIONS

The results obtained in this paper for the ^{4}He condensate fraction and the x_3 dependence of the ^{3}He kinetic energy are in contrast with recent experimental estimates. In fact, Sokol *et al.*[6,7] analyzing deep inelastic neutron-scattering measurements carried out for a 9.5% mixture at 1.4 K, and for a momentum transfer as high as 23 Å^{-1}, estimated a condensate fraction $n_0^{(4)}=18\%$ and a ^{3}He kinetic energy of approximately 10 K, basically independent of the concentration. These results are to be compared with the theoretical predictions $n_0^{(4)}\sim 10\%$ and $T_3/N_3\sim 19$ K obtained in ACA for a similar mixture.

It has been argued[6] that the main source of discrepancy with a preliminary presentation of the present results[17] is due to the use of ACA, implying the same type of local environment for the different types of atoms in the mixture. Sokol's observation is physically founded on the large zero-point motion of the ^{3}He atoms which should decrease the local density around them to a value similar to the pure ^{3}He. Obviously, the use of optimal correlations should clarify this point. However, it must be stressed that the $T=0$ DMC calculations of Ref. 39 give for the ^{3}He impurity kinetic energy $T_3=17.5$ K, i.e., 1.5 K lower value than the ACA prediction estimated by using the pure ^{4}He DMC kinetic energy ($T_4=14.3$ K).[12] On the other hand, the predicted $n_0^{(4)}$ by DMC (Ref. 42) points to an extrapolated value of 11% for a 6.6% mixture at the same temperature. A dramatic change of both $n_0^{(4)}$ and T_3 at higher concentrations would be required in order to reproduce the experimental estimates.

In conclusion, we believe that although the use of optimal correlations will certainly decrease the kinetic energy of the ^{3}He component and enhance a little the ^{4}He condensate fraction, the resulting values will be far from the present experimental analysis. A full theoretical calculation of the scattering process including final-state interactions and the experimental broadening, similar to the ones performed in pure ^{4}He,[43] is necessary in order to fully understand the experimental measurements and reliably extract kinetic energies and condensate fractions.

Summarizing, we have calculated the momentum distributions of ^{3}He-^{4}He mixtures in the framework of the HNC/FHNC equations using variational wave functions with two- and three-body correlations. These momentum distributions can be used as input for the analysis of the recently performed inelastic neutron-scattering experiments. It has been found that, at the low concentration where the mixture is stable, the Fermi statistics do not significantly modify the value of the ^{4}He condensate fraction. On the other hand, it is crucial to take into account the Fermi statistics for the stability of the mixture. The concentration dependence of the different quantities studied in the paper can be mainly explained by the decrease in the total density of the mixture when the ^{3}He concentration increases.

ACKNOWLEDGMENTS

The authors are especially indebted to J. Casulleras for his collaboration in the ^{4}He Monte Carlo calculations and to S. Moroni for several fruitful exchanges and discussions and for providing his VMC results. This research was supported in part by DGICYT (Spain) Grant No. PB95-0761, CICYT (Spain) Grant No. TIC95-0429, the agreement DGICYT (Spain)–INFN (Italy), and the Accion Integrada Hispano-Italiana 99A-1994.

APPENDIX A

In this appendix we present the HNC/FHNC equations for the mixture one-body density matrices. The sums of the nodal diagrams contributions, $N^{(3)}_{\omega_c\omega_c}$ and $N^{(\alpha)}_{\omega\omega}$, are obtained by solving the integral equations

$$N^{(\alpha)}_{\omega\omega}=\sum_{\lambda=3,4}\rho_\lambda\sum_{z,y}\,(g^{(\alpha,\lambda)}_{\omega z}-N^{(\alpha,\lambda)}_{\omega z}-\delta_{zd}|g^{(\lambda,\alpha)}_{y\omega}-\delta_{yd}), \tag{A1}$$

and

$$\begin{aligned}N^{(3)}_{\omega_c\omega_c}=&\rho_3(g_{\omega_c c}+l(k_F r_{12})/\nu-N^{(3)}_{\omega_c c}|g_{c\omega_c}+l/\nu)\\&+\rho_3(-l/\nu|2(g_{c\omega_c}+l/\nu-N^{(3)}_{c\omega_c})\\&-(g_{cc}+l/\nu-N_{cc})).\end{aligned} \tag{A2}$$

The notation $(A(r_{ij})|B(r_{jk}))$ stands for the convolution product

$$(A(r_{ij})|B(r_{jk}))=\int d\mathbf{r}_j A(r_{ij})B(r_{jk}). \tag{A3}$$

The summations over z and y (where $z,y=d,e,c$) always extend to all possible connections allowed by the diagrammatic rules of the HNC/FHNC theory.[16,17]

Besides the distribution functions $g^{(\alpha,\beta)}_{zy}(r)$ ($g^{(\alpha,\beta)}_{dd}$, $g^{(\alpha,3)}_{de}$, $g^{(3,3)}_{ee}$, and $g^{(3,3)}_{cc}$), which have been defined elsewhere,[20,26] it is necessary to introduce the auxiliary distribution functions:

$$g^{(\alpha,\beta)}_{\omega d}(r)=f^{(\alpha,\beta)}(r)\exp[B^{(\alpha,\beta)}_{\omega d}(r)], \tag{A4}$$

$$g^{(\alpha,3)}_{\omega e}(r)=g^{(\alpha,3)}_{\omega d}(r)B^{(\alpha,3)}_{\omega e}(r), \tag{A5}$$

$$g^{(3,3)}_{\omega_c c}(r)=g^{(3,3)}_{\omega d}(r)\,\frac{L_\omega(r)}{\nu}, \tag{A6}$$

where

$$B^{(\alpha,\beta)}_{\omega x}(r)=N^{(\alpha,\beta)}_{\omega x}(r)+E^{(\alpha,\beta)}_{\omega x}(r)+C^{(\alpha,\beta)}_{\omega x}(r), \tag{A7}$$

and

$$L_\omega(r)=-l(k_F r)+\nu B^{(3,3)}_{\omega_c c}(r). \tag{A8}$$

The functions $E^{(\alpha,\beta)}_{\omega d}(r)$, $E^{(\alpha,3)}_{\omega e}(r)$, and $E^{(3,3)}_{\omega_c c}(r)$ give the contributions of the elementary diagrams.

The nodal functions $N^{(\alpha,\beta)}_{\omega z}(r)$ are solutions of the following integral equations:

$$N^{(\alpha,\beta)}_{\omega x}=\sum_{\lambda=3,4}\rho_\lambda\sum_{z,y}\,(g^{(\alpha,\lambda)}_{\omega z}-N^{(\alpha,\lambda)}_{\omega z}-\delta_{zd}|g^{(\lambda,\beta)}_{yx}-\delta_{yd}), \tag{A9}$$

$$N^{(3,3)}_{\omega_c c}=\rho_3(g_{\omega_c c}-N_{\omega_c c}+l/\nu|g_{cc}). \tag{A10}$$

Finally, the functions $C_{\omega x}^{(\alpha,\beta)}(r)$ give the contribution of the *dressed* triplet correlations,

$$C_{\omega x}^{(\alpha,\beta)}(r_{12})=\sum_{\lambda=3,4}\rho_\lambda\int d\mathbf{r}_3\omega^{(\alpha,\lambda,\beta)}(r_{12},r_{13},r_{23})\times\sum_{zy}g_{\omega z}^{(\alpha,\lambda)}(r_{13})g_{yx}^{(\lambda,\beta)}(r_{32}), \tag{A11}$$

and

$$C_{\omega_c c}^{(3,3)}(r_{12})=\rho_3\int d\mathbf{r}_3\omega^{(3,3,3)}(r_{12},r_{13},r_{23})\times g_{\omega_c c}^{(3,3)}(r_{13})g_{cc}^{(3,3)}(r_{32}). \tag{A12}$$

The functions $N_{zy}^{(\alpha,\beta)}(r)$ and $C_{zy}^{(\alpha,\beta)}(r)$ have been defined in Ref. 20.

The quantities $\Gamma_\omega^{(\alpha)}$ and $\Gamma_d^{(\alpha)}$, entering the expressions of the strength factors $n_0^{(\alpha)}$, are given by

$$\begin{aligned}\Gamma_x^{(\alpha)}=&\sum_{\lambda=3,4}\rho_\lambda\int d\mathbf{r}(g_{xd}^{(\alpha,\lambda)}(r)-1-N_{xd}^{(\alpha,\lambda)}(r)-E_{xd}^{(\alpha,\lambda)}(r))+\rho_3\int d\mathbf{r}(g_{xe}^{(\alpha,3)}(r)-N_{xe}^{(\alpha,3)}(r)-E_{xe}^{(\alpha,3)}(r))\\&-(1/2)\sum_{\lambda=3,4}\rho_\lambda\int d\mathbf{r}(g_{xd}^{(\alpha,\lambda)}(r)-1+\delta_{\lambda 3}g_{xe}^{(\alpha,\lambda)}(r))(N_{xd}^{(\alpha,\lambda)}(r)+2E_{xd}^{(\alpha,\lambda)}(r))-(1/2)\rho_3\int d\mathbf{r}(g_{xd}^{(\alpha,3)}(r)-1)(N_{xe}^{(\alpha,3)}(r)\\&+2E_{xe}^{(\alpha,3)}(r))-(1/2)\sum_{\lambda=3,4}\rho_\lambda\int d\mathbf{r}(g_{xd}^{(\alpha,\lambda)}(r)+\delta_{\lambda 3}g_{xe}^{(\alpha,\lambda)}(r))C_{xd}^{(\alpha,\lambda)}(r)-(1/2)\rho_3\int d\mathbf{r}g_{xd}^{(\alpha,3)}(r)C_{xe}^{(\alpha,3)}(r)+E_x^{(\alpha)},\end{aligned} \tag{A13}$$

where $E_x^{(\alpha)}$ is the sum of the one-point elementary diagrams.[8,9,17] By setting $\rho_3=0$ $(\rho_4=0)$, expression (2.15) reduces to the pure phases Γ_x.[8,9]

APPENDIX B

In this appendix, results for the momentum distributions of the different components of the mixture at several ^{3}He concentrations are reported in the following table:

	$x_3=0.02$		$x_3=0.04$		$x_3=0.066$	
k (Å^{-1})	$n^{(4)}(k)$ (10^{-2})	$n^{(3)}(k)$ (10^{-3})	$n^{(4)}(k)$ (10^{-2})	$n^{(3)}(k)$ (10^{-3})	$n^{(4)}(k)$ (10^{-2})	$n^{(3)}(k)$ (10^{-2})
0.00	53.9037	89.7342	52.9961	96.7339	51.8615	10.5508
0.05	53.7869	89.5174	52.8810	96.6067	51.7480	10.5416
0.10	53.4385	89.4813	52.5376	96.4602	51.4095	10.5170
0.15	52.8645	89.3475	51.9718	96.3355	50.8519	10.4846
0.20	52.0749	89.2132	51.1935	96.2190	50.0848	10.4533
0.25	51.0825	4.9579	50.2154	96.0861	49.1211	10.4297
0.30	49.9035	5.1966	49.0532	9.7540	47.9763	10.4151
0.35	48.5558	5.1927	47.7248	9.7000	46.6680	1.5302
0.40	47.0590	4.9945	46.2494	9.4897	45.2153	1.5077
0.45	45.4335	4.6889	44.6470	9.1555	43.6381	1.4750
0.50	43.6997	4.3663	42.9379	8.7442	41.9563	1.4284
0.55	41.8776	4.0904	41.1417	8.3027	40.1894	1.3680
0.60	39.9864	3.8836	39.2774	7.8661	38.3560	1.2977
0.65	38.0439	3.7306	37.3623	7.4521	36.4734	1.2233
0.70	36.0664	3.5954	35.4127	7.0620	34.5574	1.1503
0.75	34.0687	3.4424	33.4431	6.6862	32.6224	1.0822
0.80	32.0639	3.2531	31.4664	6.3124	30.6811	1.0198
0.85	30.0637	3.0307	29.4943	5.9321	28.7448	0.9611
0.90	28.0787	2.7946	27.5372	5.5437	26.8239	0.9033
0.95	26.1185	2.5685	25.6046	5.1526	24.9277	0.8442
1.00	24.1919	2.3685	23.7054	4.7676	23.0649	0.7830
1.05	22.3073	2.1973	21.8480	4.3968	21.2437	0.7209

	$x_3=0.02$		$x_3=0.04$		$x_3=0.066$	
k (Å^{-1})	$n^{(4)}(k)$ (10^{-2})	$n^{(3)}(k)$ (10^{-3})	$n^{(4)}(k)$ (10^{-2})	$n^{(3)}(k)$ (10^{-3})	$n^{(4)}(k)$ (10^{-2})	$n^{(3)}(k)$ (10^{-2})
1.10	20.4731	2.0454	20.0406	4.0451	19.4722	0.6601
1.15	18.6973	1.8983	18.2913	3.7125	17.7585	0.6026
1.20	16.9880	1.7447	16.6081	3.3960	16.1104	0.5495
1.25	15.3531	1.5815	14.990	3.0915	14.5358	0.5006
1.30	13.8004	1.4145	13.4717	2.7964	13.0423	0.4547
1.35	12.3371	1.2541	12.0332	2.5110	11.6368	0.4106
1.40	10.9699	1.1095	10.6902	2.2381	10.3258	0.3675
1.45	9.7043	0.9846	9.4480	1.9821	9.1146	0.3258
1.50	8.5445	0.8770	8.3109	1.7470	8.0071	0.2864
1.55	7.4932	0.7805	7.2812	1.5352	7.0057	0.2506
1.60	6.5514	0.6892	6.3599	1.3469	6.1110	0.2194
1.65	5.7181	0.6007	5.5457	1.1809	5.3217	0.1929
1.70	4.9900	0.5173	4.8354	1.0351	4.6345	0.1704
1.75	4.3625	0.4436	4.2241	0.9081	4.0443	0.1510
1.80	3.8286	0.3842	3.7050	0.7987	3.5442	0.1338
1.85	3.3803	0.3405	3.2697	0.7063	3.1260	0.1184
1.90	3.0080	0.3101	2.9090	0.6302	2.7802	0.1049
1.95	2.7015	0.2877	2.6125	0.5688	2.4967	0.0936
2.00	2.4503	0.2678	2.3698	0.5194	2.2652	0.0846
2.05	2.2439	0.2469	2.1706	0.4789	2.0753	0.0777
2.10	2.0721	0.2247	2.0049	0.4440	1.9175	0.0724
2.15	1.9257	0.2032	1.8637	0.4119	1.7830	0.0677
2.20	1.7969	0.1849	1.7391	0.3812	1.6640	0.0630
2.25	1.6788	0.1711	1.6246	0.3513	1.5543	0.0581
2.30	1.5662	0.1610	1.5153	0.3224	1.4492	0.0528
2.35	1.4556	0.1521	1.4076	0.2951	1.3453	0.0477
2.40	1.3447	0.1418	1.2995	0.2694	1.2408	0.0432
2.45	1.2325	0.1287	1.1901	0.2452	1.1349	0.0393
2.50	1.1194	0.1133	1.0797	0.2221	1.0280	0.0360
2.55	1.0063	0.0977	0.9694	0.1997	0.9213	0.032
2.60	0.8949	0.0842	0.8608	0.1780	0.8165	0.0297
2.65	0.7871	0.0743	0.7559	0.1574	0.7155	0.0264
2.70	0.6849	0.0676	0.6567	0.1384	0.6201	0.0230
2.75	0.5901	0.0627	0.5648	0.1215	0.5321	0.0198
2.80	0.5043	0.0575	0.4818	0.1068	0.4528	0.0171
2.85	0.4283	0.0508	0.4085	0.0942	0.3830	0.0150
2.90	0.3627	0.0428	0.3454	0.0832	0.3232	0.0135
2.95	0.3074	0.0346	0.2923	0.0732	0.2731	0.0122
3.00	0.2618	0.0280	0.2487	0.0638	0.2321	0.0110
3.05	0.2250	0.0238	0.2136	0.0550	0.1992	0.0096
3.10	0.1957	0.0219	0.1858	0.0471	0.1733	0.0081
3.15	0.1726	0.0212	0.1638	0.0403	0.1528	0.0066
3.20	0.1541	0.0201	0.1463	0.0347	0.1365	0.0055
3.25	0.1389	0.0178	0.1318	0.0303	0.1230	0.0047
3.30	0.1257	0.0141	0.1193	0.0266	0.1112	0.0043
3.35	0.1137	0.0102	0.1078	0.0234	0.1003	0.0041
3.40	0.1020	0.0071	0.0966	0.0203	0.0897	0.0038
3.45	0.0904	0.0057	0.0854	0.0174	0.0790	0.0033
3.50	0.0786	0.0060	0.0740	0.0147	0.0682	0.0027

[1] *Momentum Distributions*, edited by R. N. Silver and P. E. Sokol (Plenum, New York, 1989).
[2] H. R. Glyde, *Excitations in Liquid and Solid Helium* (Clarendon, Oxford, 1994).
[3] T. R. Sosnick, W. M. Snow, P. E. Sokol, and R. N. Silver, Europhys. Lett. **9**, 707 (1989).
[4] T. R. Sosnick, W. M. Snow, and P. E. Sokol, Phys. Rev. B **41**, 11 185 (1990).
[5] P. E. Sokol, K. Skold, D. L. Price, and R. Kleb, Phys. Rev. Lett. **54**, 909 (1985).
[6] Y. Wang and P. E. Sokol, Phys. Rev. Lett. **72**, 1040 (1994).
[7] R. T. Azuah, W. G. Stirling, J. Mayers, I. F. Bailey, and P. E. Sokol, Phys. Rev. B **51**, 6780 (1995).
[8] E. Manousakis, V. R. Pandharipande, and Q. N. Usmani, Phys. Rev. B **31**, 7022 (1985).
[9] A. Fabrocini, V. R. Pandharipande, and Q. N. Usmani, Nuovo Cimento D **14**, 469 (1992).
[10] R. M. Panoff and P. A. Whitlock, in *Momentum Distributions*, edited by R. N. Silver and P. E. Sokol (Plenum, New York, 1989).
[11] P. Whitlock and R. M. Panoff, Can. J. Phys. **65**, 1409 (1987).
[12] J. Boronat and J. Casulleras, Phys. Rev. B **49**, 8920 (1994).
[13] D. M. Ceperley and E. L. Pollock, Phys. Rev. Lett. **56**, 351 (1986).
[14] Q. N. Usmani, S. Fantoni, and V. R. Pandharipande, Phys. Rev. B **26**, 6123 (1982).
[15] E. Manousakis, S. Fantoni, V. R. Pandharipande, and Q. N. Usmani, Phys. Rev. B **28**, 3770 (1983).
[16] A. Fabrocini and A. Polls, Phys. Rev. B **26**, 1438 (1982).
[17] J. Boronat, A. Polls, and A. Fabrocini, in *Condensed Matter Theories*, edited by V. C. Aguilera-Navarro (Plenum, New York, 1990), Vol. 5, p. 27.
[18] W. Lee and B. Goodman, Phys. Rev. B **24**, 2515 (1981).
[19] E. Krostcheck and M. Saarela, Phys. Rep. **232**, 1 (1993).
[20] J. Boronat, A. Polls, and A. Fabrocini, J. Low Temp. Phys. **91**, 275 (1993).
[21] M. Boninsegni and D. M. Ceperley, Phys. Rev. Lett. **74**, 2288 (1995).
[22] A. Fabrocini, L. Vichi, F. Mazzanti, and A. Polls, Phys. Rev. B **54**, 10 035 (1996).
[23] A. Polls, F. Mazzanti, J. Boronat, F. Dalfovo, and A. Fabrocini, in *Recent Progress in Many-Body Theories*, edited by E. Schachinger, H. Mitter, and H. Sormann (Plenum, New York, 1995), Vol. 4, p. 101.
[24] M. L. Ristig and J. W. Clark, Phys. Rev. B **14**, 2875 (1976).
[25] S. Fantoni, Nuovo Cimento A **44**, 191 (1978).
[26] A. Fabrocini and A. Polls, Phys. Rev. B **25**, 4533 (1982).
[27] Q. N. Usmani, B. Friedman, and V. R. Pandharipande, Phys. Rev. B **25**, 4502 (1982).
[28] A. Fabrocini and S. Rosati, Nuovo Cimento D **1**, 567 (1982).
[29] L. Oddi and L. Reatto, Nuovo Cimento D **11**, 1679 (1989).
[30] R. A. Aziz, V. P. S. Nain, J. S. Carley, W. L. Taylor, and G. T. McConville, J. Chem. Phys. **70**, 4330 (1979).
[31] R. M. Panoff and J. Carlson, Phys. Rev. Lett. **62**, 1130 (1989).
[32] J. Boronat, A. Fabrocini, and A. Polls, J. Low Temp. Phys. **74**, 347 (1989).
[33] A. Fabrocini and A. Polls, Phys. Rev. B **30**, 1200 (1984).
[34] R. D. Guyer and M. D. Miller, Phys. Rev. B **22**, 142 (1980).
[35] S. Moroni (private communication).
[36] E. Manousakis, V. R. Pandharipande, and Q. N. Usmani, Phys. Rev. B **43**, 13 587 (1991).
[37] S. Moroni, G. Senatore, and S. Fantoni, Phys. Rev. B **55**, 1040 (1997).
[38] W. N. Snow, Y. Wang, and P. E. Sokol, Europhys. Lett. **19**, 403 (1992).
[39] J. Casulleras, J. Boronat, and A. Polls, Czech. J. Phys. **46**, Suppl. S1, 271 (1996).
[40] A. Fabrocini, S. Fantoni, S. Rosati, and A. Polls, Phys. Rev. B **33**, 6057 (1986).
[41] R. A. Sherlock and D. O. Edwards, Phys. Rev. A **8**, 2744 (1973).
[42] S. Moroni and M. Boninsegni, Czech. J. Phys. **46**, Suppl. S1, 271 (1996).
[43] F. Mazzanti, J. Boronat, and A. Polls, Phys. Rev. B **53**, 5661 (1996).